HEFAT2014
10th International Conference on Heat Transfer, Fluid Mechanics and Thermodynamics
14 – 16 July 2014
Orlando, Florida

EXPERIMENTAL ANALYSIS OF REFRIGERATED TRUCK THERMAL BEHAVIOUR

Kayansayan N.*, Ezan M.A., Alptekin E., Yıldız A., and, Günes T.
*Author for correspondence
Department of Mechanical Engineering,
Dokuz Eylül University,
Izmir, 35397
Turkey,
E-mail: nuri.kayansayan@deu.edu.tr

ABSTRACT

This study mainly focuses on experimental investigation of ceiling-slot ventilated enclosures for determining the airflow and thermal characteristics. The experimental prototype has the dimensions of 8.33 m (length) x 2.50 m (height) x 2.46 m (width) and the cooled air is injected into the container through a half-width slot positioned at the centre of front surface and close to the ceiling. The prototype is positioned inside of a climatic test chamber having dimensions of 14 m (length) x 5 m (width) x 6.5 m (height). The temperature and the relative humidity of the test chamber may be varied within limits of (-20°C and +50°C), and (5% and 95%) respectively. The air velocity at the slot exit is varied by changing the fan speed so that two different Reynolds numbers $4.3x10^5$ and $7.86x10^5$ are studied in the analysis. In experiments, the system at specified inside, outside and airflow conditions is approximately run for two hours to establish steady-state conditions. In recording data, the system data is divided into two groups: 1. The cooling unit data that includes refrigerant side volumetric flow rate, the pressure and temperature at the inlet and outlet of compressor, condenser and evaporator. Additionally, temperature and volumetric flow rate of air through the condenser, and the fuel consumption of the engine are also recorded. 2. The container data covers air velocity at the slot exit, and a total of 110 thermocouples measure the surface temperatures of all surfaces (inside and outside) of the container and local temperature variation of the airflow. Measurements carried out at both sides (air side and refrigerant side) to validate the data with an accuracy band ±6.5% of the air side measurements. The thermal performance of ventilation in the container is measured by a non-dimensional temperature distribution, θ_x at a particular cross-section. As a result of measured data, conventional COP of the system and COP_f based on fuel consumption rate are also presented.

NOMENCLATURE

A	[m^2]	Cross-sectional area
c_p	[J/kgK]	Specific heat of air
D_H	[m]	Hydraulic diameter of the inlet section, $D_H=4A/P$
H	[m]	Height of the container
h	[kJ/kg]	Enthalpy
k	[W/mK]	Thermal conductivity
L	[m]	Length of the container
l	[m]	Evaporator size
P	[m]	Perimeter
p	[Pa]	Pressure
Q	[W]	Heat transferred by a surface or by evaporator
Re	[-]	Reynolds number, $Re = \rho V_{inj} D_H/\mu$
T	[K]	Local temperature
T_x	[K]	Enthalpy averaged air temperature of a plane at x
t	[s]	Time
W	[m]	Container width
u, v, w	[m/s]	Velocity components
x, y, z	[m]	Cartesian axis directions

Special characters

θ	[-]	Non-dimensional local temperature
θ_x	[-]	Non-dimensional and enthalpy based temperature of a plane at x
μ	[kgm/s^2]	Dynamic viscosity
ϑ	[m^3/s]	Flow rate
ν	[m^2/s]	Kinematic viscosity
ρ	[kg/m^3]	Density of air

Subscripts

a	Air
$cond$	Condenser
$conda$	Condenser air side
$condR$	Condenser refrigerant side
ev	Evaporator
eva	Evaporator air side
evR	Evaporator refrigerant side
f	fuel
i	Inside
in	Evaporator inlet
inj	Evaporator exit
o	Surroundings

INTRODUCTION

In carrying perishable goods, maintaining unchanged thermal conditions inside the truck until the product is delivered has direct input on the final quality of the transported goods. Literature review however indicates that refrigerated containers having volumes larger than 50m^3 are rarely investigated and very scarce experimental data is published. In accord with the agreement on the international carriage of perishable food stuffs and on the special equipment to be used for such carriage (ATP), Chatzidakis et al. [1] provides testing procedure for refrigerated equipment, and indicates that alternative testing procedures yield incorrect test results. Rodriquez-Bermejo et al. [2] experimentally measured temperature distribution inside of a container with dimensions of 2620 mm x 2184 mm x 2270 mm. In experiments, the cooling system is located at the top of the compartment and several cooling modes, and the onset of defrosting are studied. Tso et al.[3] experimentally studied the heat transfer effect of air curtain or presence of plastic strip curtain at the side door of a refrigerated container having dimensions of 2.84m(length)x1.64m(width)x1.54m(height).

As shown in Figure 1, this study presents experimental analysis carried out for a ceiling slot-ventilated enclosure with the injection and the suction sections are on the same but at different sides of the cooling device. The evaporator of the cooling device is located at the top of the front surface and is at the symmetry line of the container (see Fig.2). The aim of the work is to determine the airflow temperature distributions at different flow Reynolds numbers inside the container and also evaluate the thermal performance of the entire system.

Figure 1 Experimental prototype for refrigerated truck

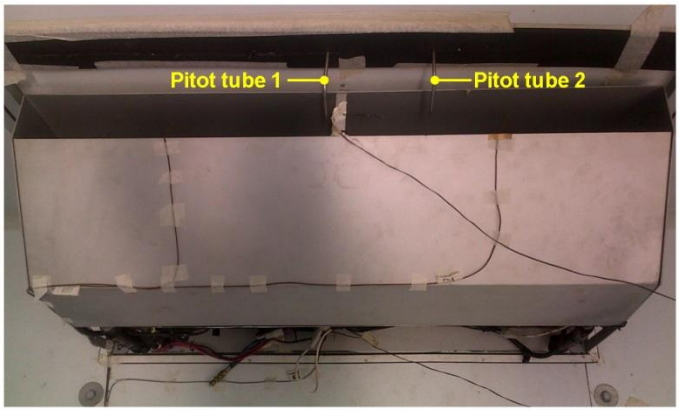

Figure 2 Evaporator and pitot tube locations

EXPERIMENTAL SETUP AND INSTRUMENTATION

The experimental system is assembled by two basic sub-sections: 1.The cooling system, 2.The refrigerated container. As depicted in Figure 3, the cooling system is self-powered by a Bock brand 15 kW diesel engine. The engine delivers power to open-type, two-cylinder reciprocating compressor for compressing refrigerant R404A which is the working fluid of the system. Each cylinder has 60 mm of bore and 49 mm of stroke, and provides 24.1 m^3/h volume flow rate at a speed of 1450 rpm. The cooling system is also equipped with a 7.5kW electric motor powered by city electricity network and supplies energy to the refrigeration system when the truck is at a parking lot with all engines are at off position. The evaporator section of the unit penetrates into the container at the front face and located at the container symmetry line. The slot dimension at the evaporator exit is 123 cm x 9.6 cm, and at the suction side is 123 cm x 23.4 cm. A thermostatic expansion valve with an orifice diameter of 3.5 mm, providing 8.8 kW of refrigeration for R404A is used in the system.

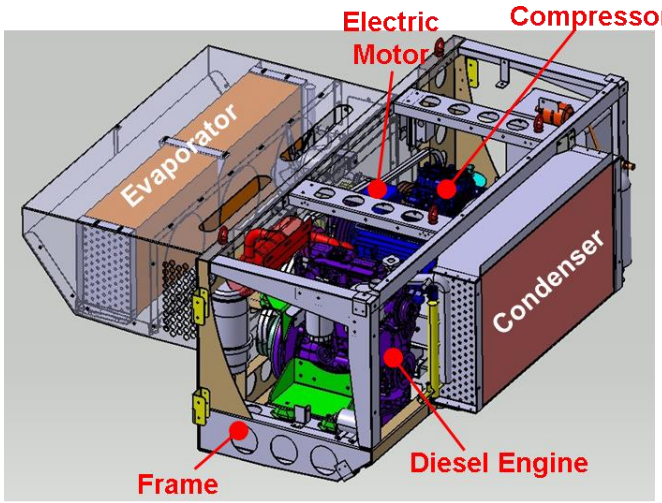

(a) Isometric view

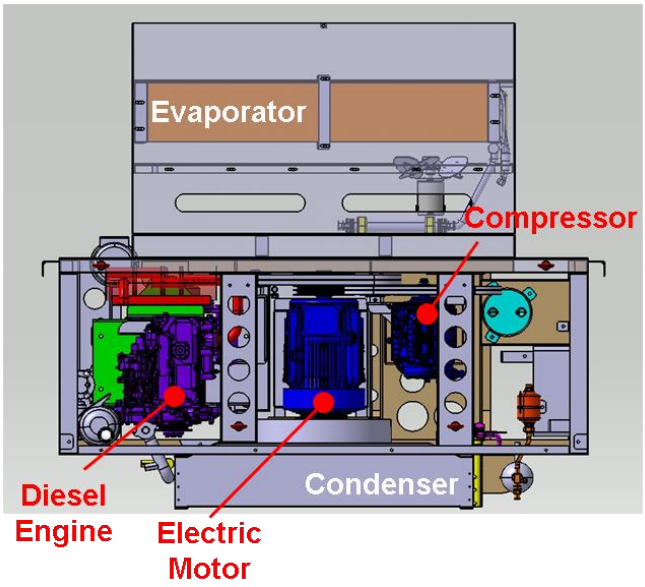

(b) Top view

Figure 3 Main components of cooling unit

The evaporator and the condenser both are fin-and-tube type heat exchangers constructed by aluminum fins and copper tubes. The frontal area of both exchangers is 0.39 m^2, and the tube pitch in flow direction is 22 mm, perpendicular to the low is 25 mm. The distance between fins is 2.2 mm for condenser and 3.2 mm for the evaporator. The air side of both evaporator and the condenser is furnished with axial fans for circulating the air. In experiments, to vary the airflow rate inside the container, a variable speed fan is used at the evaporator side. In addition, the refrigeration system includes a dryer, a sight glass, a pressure stat, a solenoid valve, and a pressure regulator. Having the dimensions of 2.46 m (width) x 2.5 m (height) x 8.33 m (length), the refrigerated container is constructed in accord with ISO standards and is furnished with two-panel door opening at the rear and a single door at the side. The container wall thickness values are given in Table 1. Moreover, the container is furnished with thermocouple holding frames of identical size. The frames can be moved in the container so that the local temperature variation of airflow can be measured.

Table 1 Insulation thickness of container walls

Wall	Front	Rear	Top	Bottom	Side
Thickness (mm)	80	80	100	120	85

A slot with dimensions of 345 mm x 1240 mm located at the symmetry line of the front surface allows the evaporator section of the cooling system to be inserted into the container. At the top surface, a slot with dimensions of 1240 mm x 40 mm accommodates the mounting system for pitot-tube which measures the air velocity at the evaporator exit. All surfaces providing any insertions are made air leak free by epoxy glue.

As shown in Figure 4, the refrigeration flow rate of R404A flowing through the refrigeration system is metered by KROHNE H250/M9 variable area flow meter. The meter has a sensitivity of ±1.6% of the full range and located between the receiver tank and the expansion valve of the system.

Figure 4 Flowmeter installation for refrigeration system

In determining the capacity rates of the condenser, the evaporator, and the compressor, three pressure transducers of CAREL type model: SPKT0013R/33R are used and sequentially mounted at the exits of the evaporator, compressor and the condenser. Similarly, pressure difference across nozzles is detected by KIMO type model: CP-101/A0 pressure transmitter. As presented in Figure 5a, the airflow rate through the condenser is measured by four nozzles that are manufactured and calibrated in accord with ANSI/ASHRAE 51-07 standards [4].

(a) Distribution of nozzles at the condenser inlet

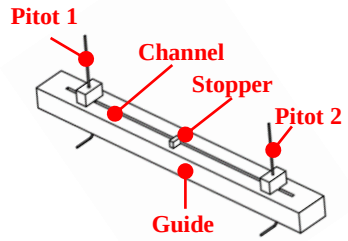

(b) Flow measurement at the evaporator outlet

Figure 5 Use of nozzle and pitot tube in experiments

In addition, air velocities at the evaporator exit are measured by Pitot tubes moving horizontally in a guided channel which is fixed into the slot at the ceiling of the container (Fig. 5b). These pitot tubes are positioned at the centerline of the evaporator exit. As indicated in Figure 6, the same pressure transmitter used for nozzle flow rates records the pressure difference of pitot tubes.

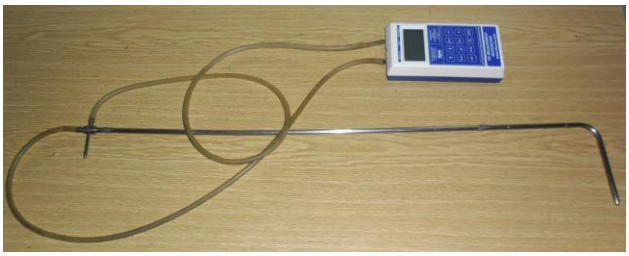

Figure 6 Pressure transmitter with pitot tube

To record the temperature of refrigerant at the inlet and outlet of evaporator, condenser and the compressor, temperature sensors of type PT-100 are utilized. The airflow temperatures are measured by 24 AWG copper-constantan (Type T) thermocouple elements. To determine the cross-sectional temperature distribution at a particular container location three identical moving frames are built. As shown in Figure 7a, each frame sub-divides the cross-section into 15 smaller regions with a thermocouple at the centre. The thermocouple distribution for the top, bottom, lateral, front and rear surfaces including the inside and outside wall surfaces is illustrated in Figure 7b and Figure 7c. Together with the thermocouples located on the inside and outside wall surfaces, the experimental container is equipped with a total of 110 thermocouples. The temperatures are recorded by Agilent type, model: 34970A data acquisition system with a recording accuracy of ±1.5°C. The measuring range and accuracy of other instruments used in the analysis is indicated in Table 2.

Table 2 Instruments and accuracies

Instrument	Model	Range	Accuracy
Flow meter	KROHNE H250/M9	61 to 610L/h	±1.6%
Pressure transducer	CAREL SPKT	-1 to 9.3 bar or 0 to 34.5 bar	±1.2%
Temperature measurement	T-Type 24AWG	-200 to 204°C	±0.5°C
Pressure transmitter	KIMO CP-101	-500 to 1000Pa	±1.5%
Fuel consumption scale	Rothenberger	0.0 to 120 kg	±0.5%

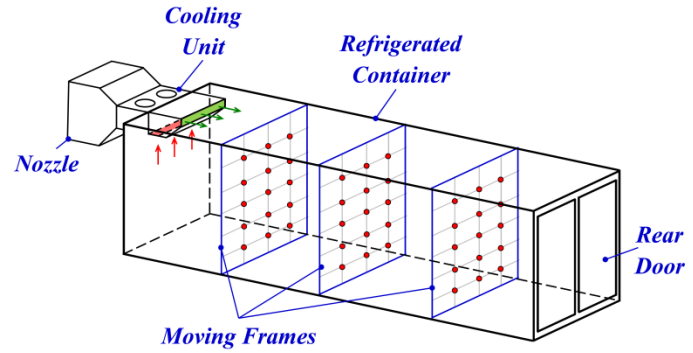

(a) Moving frames

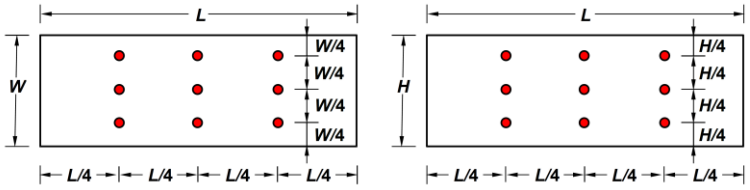

(b) Top, bottom and lateral walls – *Inner surfaces*

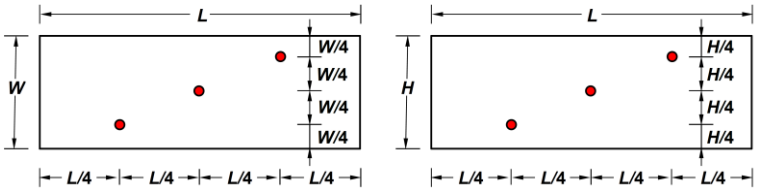

(b) Top, bottom and lateral walls – *Outer surfaces*

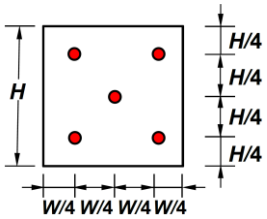

(c) Front and lateral walls *Inner surfaces*

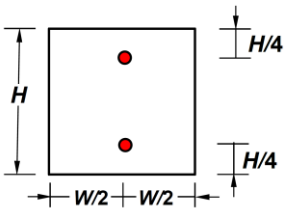

(c) Front and lateral walls *Outer surfaces*

Figure 7 Temperature measurements and thermocouple locations for the refrigerated container

EXPERIMENTAL PROCEDURE AND RESULTS

In performing experiments, the container is placed inside a climatic test chamber at which surroundings temperature and relative humidity may be controlled within limits -20°C to +50°C and 5% to 95% respectively. First the surroundings temperature in the chamber is brought to +40°C with the relative humidity at 70%, then the fan speed is adjusted so that two different Reynolds numbers of airflow at the evaporator exit is analyzed in experiments. The refrigeration unit is switched on and the air inside the container is allowed to cool down until the temperatures reached steady-state. The steady-state conditions are assumed to be obtained when the rate of change of air temperature at the evaporator exit is less than 0.15K/min ($DT / Dt \le 0.15$K/min). Figure 8 illustrates time-wise variation of air temperature at the evaporator inlet and outlet for Reynolds number 7.86×10^5. According to this figure, it takes about two hours for the system to attain a steady temperature that is usually higher than the set point temperature.

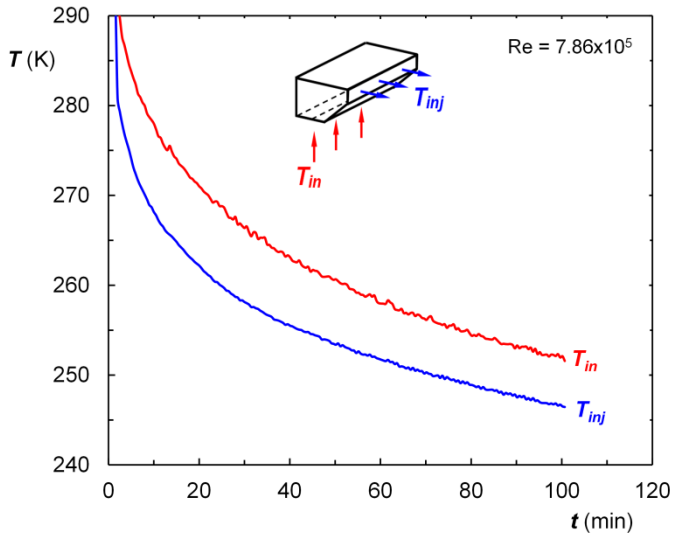

Figure 8 Time-wise variation of air temperature at the evaporator inlet and outlet - T_o = +40°C

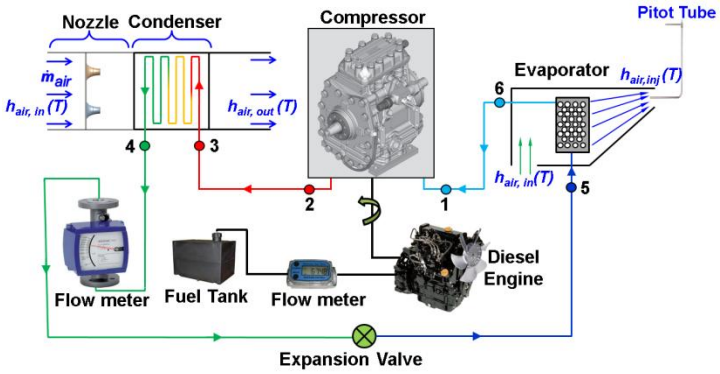

(a) Schematic of experimental cooling unit

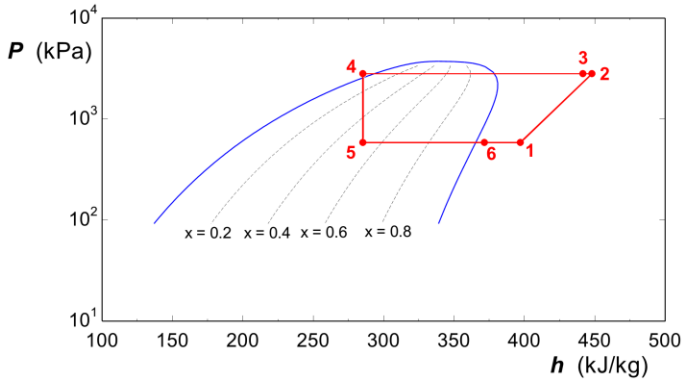

(b) *h-p* diagram for refrigeration cycle

Figure 9 Cooling unit and instrumentation

Figure 9 shows schematically the test set-up and the related *h-p* diagram of the refrigeration cycle. In data recording, two sets of data; one for the refrigeration unit, and the other for the container, are collected simultaneously at 10-second time interval. The experiments are repeated 4 times by changing airflow Reynolds number and the surroundings temperature. Table-3 summarizes these 4 cases.

Table 3 Working parameters

Experimental case	Ambient Temperature (°C)	Storage Temperature (°C)	Airflow Reynolds no.
1	+40	-20	$4.3\text{x}10^5$
2	+40	-20	$7.86\text{x}10^5$
3	+20	-20	$4.3\text{x}10^5$
4	+20	-20	$7.86\text{x}10^5$

For refrigeration unit, the enthalpy values at several states on *h-p* diagram in Fig. 9, and the specific volume of R404A at state 4 are determined by EES (Engineering Equation Solver) software [5]. Together with the volume flow rate measured by KROHNE device, the mass flow rate of refrigerant is:

$$\dot{m}_R = \vartheta_4 / v_4 \tag{1}$$

In accord with the collected data on the refrigerant side, the evaporator, the condenser and the compressor capacities are computed as following,

$$\dot{Q}_{evR} = \dot{m}_R \left(h_6 - h_4\right) \tag{2}$$

$$\dot{Q}_{condR} = \dot{m}_R \left(h_3 - h_4\right) \tag{3}$$

$$\dot{W}_{comp} = \dot{m}_R \left(h_2 - h_1\right) \tag{4}$$

To compute the evaporator capacity with respect to data on the air side, the mass flow rate of air is determined by pitot-tube measurements. Since the pitot-tube is positioned parallel to the injected air flow at the centre line of evaporator outlet, then the area weighted mass flow rate of air is:

$$\dot{m}_{ai} = \rho_a \sum_j V_j A_j \tag{5}$$

The injection velocity of air is measured at 8 points, and the mass flow rate is calculated accordingly. With respect to measured values of T_{inj} and T_{in}, the air side evaporator capacity becomes,

$$\dot{Q}_{eva} = \dot{m}_{ai} c_{pa} \left(T_{inj} - T_{in}\right) \tag{6}$$

The heat gain by the refrigerant (eq. (2)) at the evaporator is compared with the heat loss of container air (eq. (6)). As illustrated in Figure 10, the heat transfer rate difference between the two sides is within ±5% range of refrigerant side heat transfer rate and is considered to be acceptable for engineering analysis.

As explained in reference [5], the volumetric flow rate of air through four identical and elliptical nozzles is calculated by considering the geometric parameters and the pressure drop across the nozzles. Hence, the mass flow rate of air through the condenser is as following,

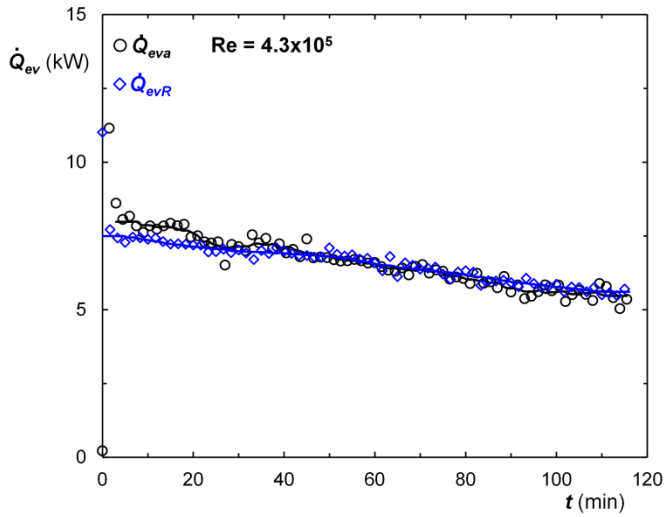

Figure 10 Comparison of heat rates computed both sides of the evaporator at T_o = +40°C

$$\dot{m}_{ao} = \rho_{ao} \vartheta_a \tag{7}$$

Then the condenser heat capacity rate with respect to parameters measured at the air side is,

$$\dot{Q}_{conda} = \dot{m}_{ao} c_{pa} \left(T_{ex} - T_o\right) \tag{8}$$

Similar to evaporator measurements, the heat rates calculated at both sides of the condenser may be compared.

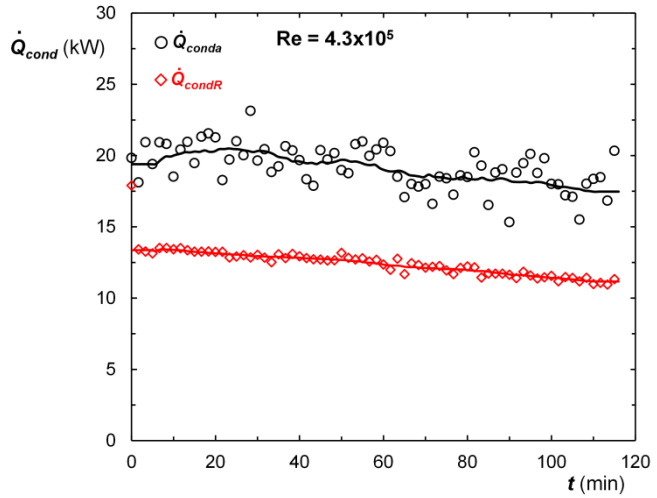

Figure 11 Experiment case 1: Evaluation of condenser heat rate by measurements on air and refrigerant sides at $T_o = +40°C$

Considering the data after steady-state conditions reached, Figure 11 shows variation of heat rate capacities of the condenser measured at both sides. As can be seen by this figure, the air-side measurements result with higher heat rates. The difference between the two measurements is due to heat rejection of cooling water system of the diesel engine driving the compressor. The condenser used in experiments furnished with seven rows of tubes in the flow direction. However, the last two rows are not part of refrigeration cycle and totally used for rejecting the cooling water heat generated by the engine. For experimental runs; cases 1 and 2, the engine side cooling water measurements indicate that the water temperature averagely decreases by $\Delta T = 2.9°C$ at a mass flow rate of $\dot{m}_w = 0.6$ kg/s. In Fig. 11, 60 minutes after the steady-state conditions is reached, the difference between the data shows that 6.7 kW of heat is rejected by cooling water at the condenser. For the same conditions, however, measurements at the cooling water side shows that the rejected heat rate is supposed to be 7.14 kW.

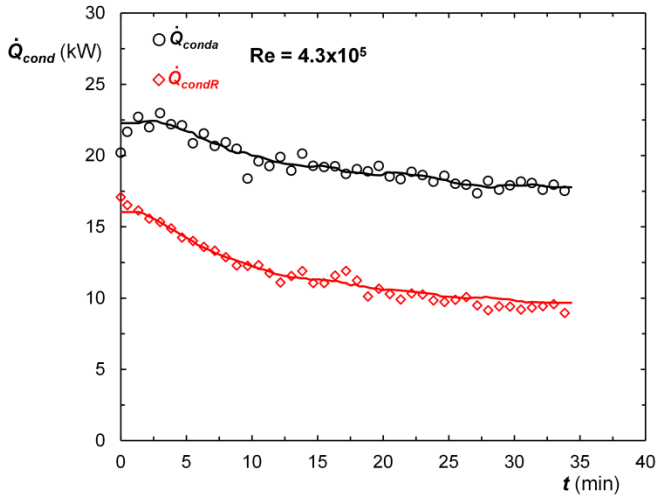

Figure 12 Experiment case 3: Evaluation of condenser heat rate by measurements on air and refrigerant sides at $T_o = +20°C$

As in Figure 12, for case 3 at which the surroundings temperature is 20°C, the difference between two data at 20 minutes after steady-state has reached is 8.75 kW. However measurements at the cooling water side indicates that water flow rate is $\dot{m}_w = 0.3$ kg/s and the temperature change through the condenser is $\Delta T = 7.9°C$ which yields a heat rejection rate of 9.15 kW. Hence, the deviations for the entire set of experiments being in a range of ±6.5% the air-side heat capacity measurements are considered to be acceptable for present analysis.

The effect of surroundings temperature and the air flow Reynolds number on the cooling unit performance is studied in Figure 13 where *COP* indicates the coefficient of performance of the refrigeration system and is defined as,

$$COP = \frac{\dot{Q}_{evR}}{\dot{W}_{comp}} \qquad (9)$$

In this expression all the heat rates and the power consumed by the compressor are evaluated respect to data at the refrigeration side. Surroundings temperature definitely affects the performance of the system, and as the temperature difference between outside and inside decreases the *COP* of the system increases. In Fig. 13, decrease of surroundings temperature from 40°C to 20°C increases *COP* by 25-percent.

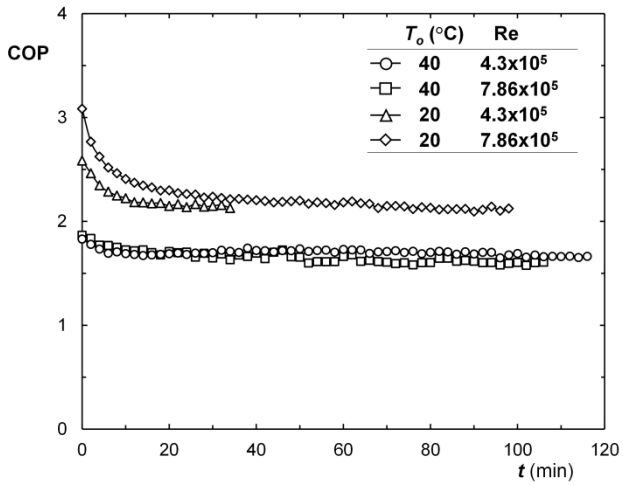

Figure 13 COP evaluation with respect to refrigerant side measurements

No traceable effect of air flow Reynolds number inside the container on the performance of the cooling unit is noted. However, as shown in Figure 14, Reynolds number of air flow affects the temperature distribution inside the container.

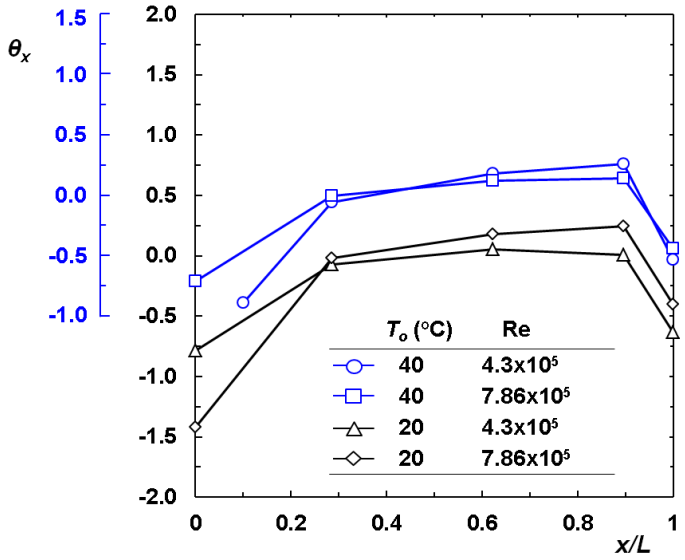

Figure 14 Local variation of air temperature and existence of hot spots

In Fig. 14, θ_x is the non-dimensional air temperature and defined as,

$$\theta_x = \frac{T_{in} - T_x}{T_{in} - T_{inj}} \tag{10}$$

where, T_x indicates the area averaged of air temperature at a particular container cross-section and is evaluated as,

$$T_x = \frac{\sum_j A_j T_j}{\sum_j A_j} \tag{11}$$

The cross-sectional averaged temperature at a particular location is evaluated by the data at 15 points on the temperature grids. At steady-state conditions, the air temperatures at the evaporator inlet and outlet are constant, and then the difference $\left(T_{in} - T_{inj}\right)$ is also constant. Increase in θ_x-curve refers to the decrease of local temperature T_x in a region close to the rear section of the container. As a result of separation of air jet from the ceiling, a circulation zone with lower average temperature exists in this region. Close to the rear door, however, air temperature again increases. The existence of negative θ_x values in both front and rear sections demonstrates the occurrence of hot spots in these regions.

Finally, the fuel consumption rate of the system is measured and then the overall performance coefficient COP_f is computed for steady-state conditions. Since the cooling system is self-driven system, the effect of environmental conditions and the storage temperature on the fuel consumption rate is of engineering interest. The system overall COP_f value based on fuel consumption rate is defined as,

$$COP_f = \frac{\dot{Q}_{evR}}{\dot{Q}_f} \tag{12}$$

where $\dot{Q}_f$ indicates the heat energy released by the diesel fuel at atmospheric conditions. For all experimental cases studied at steady-state conditions, the amount of fuel consumed is registered at five minutes intervals by an electronic scale having a resolution of 5 g. Figure 15 illustrates the variation of fuel consumption as a function of time for the engine under use and explains that linear distribution yields constant fuel consumption rate over the time interval of experiments.

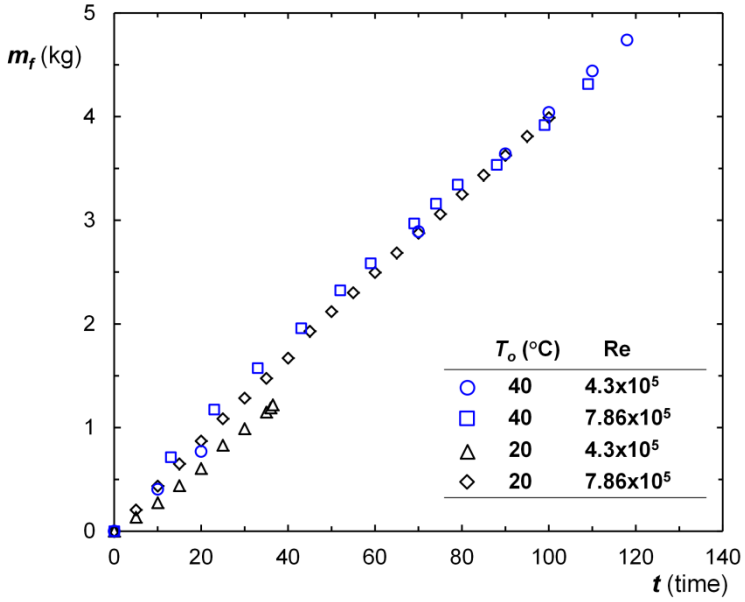

Figure15 Time-wise variation of fuel consumption

For four cases of experimental runs, Table-4 summarizes the averaged energy released rates for a heating value of 42700 kJ/kg-fuel. Results show that for a storage temperature of $T_i = -20^{\circ}\mathrm{C}$, and at severe environmental conditions ($T_o = +40^{\circ}\mathrm{C}$), the COP_f of the system drops down to 0.2. However, as the temperature difference between inside and outside decreases, COP_f assumes higher values.

Table 4 Fuel consumption rates and overall COP_f values

Experimental case	$\dot{Q}_{evR}$ (kW)	$\dot{Q}_f$ (kW)	COP_f
1	6.552	28.57	0.229
2	5.720	28.40	0.201
3	7.186	23.78	0.302
4	8.350	28.40	0.294

CONCLUSION

Thermal behavior of a full sized container of refrigerated truck is experimentally studied. The container is positioned inside of a climatic test chamber by which the temperature and the humidity of surroundings may be modified to generate moderate or severe atmospheric conditions for the cooling system. For the experimental cases studied, air inside the container assumes a fixed value of -20°C at steady state conditions. However, the air flow Reynolds number, and the temperature of surroundings have been altered for each case. The experimental runs for the cooling unit include data both at the air side and at the refrigerant side. Comparison of both sides measured data reveals an uncertainty band $\pm 6.5\%$ of air side measurements. The performance of the refrigeration unit is mainly affected by the temperature difference between the outside and the container inside temperature. Reducing the temperature difference by 34-percent increases the system *COP* by 25-percent. In the analysis, the fuel consumption rate and the corresponding overall COP_f is also evaluated. The lengthwise variation of air temperature inside the container indicates the occurrence of circulation zone close to the rear region. Further future work may be carried out to investigate occurrence of hot spots in front and in rear regions of the container.

Acknowledgement

This research is supported by Republic of Turkey Ministry of Science, Industry and Technology under the grant number: 01114.STZ.2011-2 and Dokuz Eylül University Scientific Research Foundation Grant BAP-Project number: 2013.KB.FEN.9.

REFERENCES

[1] S.K. Chatzidakis, and K.S. Chatzidakis, Refrigerated transport and environment, Int. J. Energy Research, Vol.28, 2004, pp. 887–897.

[2] J. Rodriguez-Bermejo, P. Barreiro, J.I. Robla, and L. Ruiz-Garcia, Thermal study of a transport container, J. Food Engineering, Vol.80, 2007, pp. 517–527.

[3] Tso, C.P., Yu, S.C.M., Poh, H.J., and Jolly, P.G., Experimental study on the heat and mass transfer characteristics in a refrigerated truck, Int. J. Refrigeration, Vol.25, 2002, pp. 340-350.

[4] ANSI /AMCA Standard 210-07, ANSI/ASHRAE 51-07, Laboratory Methods of Testing Fans for Certified Aerodynamic Performance Rating.

[5] S.A. Klein and G.F. Nellis, Mastering EES, F-Chart Software, 2013.